UNCLASSIFIED

[redacted]

Copy 28
RM E56E09

NACA RM E56E09

FOR REFERENCE

NOT TO BE TAKEN FROM THIS ROOM

CAT. NO. 1935 LIBRARY BU...

By authority of NASA CCN 113 Date 6-28-67

UNCLASSIFIED

CLASSIFICATION CHANGED

RESEARCH MEMORANDUM

[redacted]

EXPERIMENTAL INVESTIGATION OF MARQUARDT SHOCK-POSITIONING CONTROL UNIT ON A 28-INCH RAM-JET ENGINE

Stamped per auth of NASA list of NOFORN Pub, dtd Jan 1961

By R. Crowl, W. R. Dunbar, and C. Wentworth

Lewis Flight Propulsion Laboratory
Cleveland, Ohio

Special Release stamp added by auth B. A. Mulcahy per ... dtd 4-25-58

Declassified by authority of NASA
Classification Change Notice
No. 113 dated June 28, 1967.

NOT TO BE REFERENCED, OR GIVEN FURTHER DISTRIBUTION WITHOUT APPROVAL OF NACA.

REVIEW COPY

CLASSIFIED DOCUMENT

This material contains information affecting the National Defense of the United States within the meaning of the espionage laws, Title 18, U.S.C., Secs. 793 and 794, the transmission or revelation of which in any manner to unauthorized person is prohibited by law.

NATIONAL ADVISORY COMMITTEE
FOR AERONAUTICS
WASHINGTON

[redacted]

UNCLASSIFIED

AVAILABLE FROM NASA TO U. S. GOV'T. AGENCIES -[U.B]
AND U. S. GOV'T. CONTRACTORS ONLY
UNCLASSIFIED

NASA Technical Library
3 1176 01435 8528

 [redacted]

(Stamped pursuant to NASA list of 116 FoK'n)
Pub. date Jan 1966

CLASSIFICATION CHANGED
UNCLASSIFIED
...ity of NASA ... #113
Date 6-28-62
by ... 2-22-63

NATIONAL ADVISORY COMMITTEE FOR AERONAUTICS

RESEARCH MEMORANDUM

EXPERIMENTAL INVESTIGATION OF MARQUARDT SHOCK-POSITIONING CONTROL UNIT ON A 28-INCH RAM-JET ENGINE

By R. Crowl, W. R. Dunbar, and C. Wentworth

4051

SUMMARY

The results of an experimental investigation of a Marquardt Aircraft Company pneumatic proportional-plus-integral shock-positioning control unit on a ram-jet engine are presented. The investigation was conducted on a MA-20B3 ram-jet engine at a flight Mach number of 2.5 over a range of altitudes from 50,000 to 65,000 feet at zero, 7°, and zero to 7° angles of attack.

The control unit satisfactorily maintained the set engine operating point at zero angle of attack for all altitudes tested and thereby indicates feasible application of a practical proportional-plus-integral control unit on a full-scale ram-jet engine.

The control unit limited (reached a maximum output) at a 7° angle of attack for altitudes of 60,000 and 65,000 feet. This was due to the shift in the static characteristics of the control pressure (with respect to fuel flow) that occurred at angle of attack.

INTRODUCTION

Previous experimental investigations (refs. 1 and 2) have demonstrated that shock-positioning controls utilizing proportional-plus-integral control action can provide fast stable controls for a ram-jet engine. In each of these earlier tests, the control functions were performed by an electronic analog computer which was never intended for actual flight applications.

As part of the U. S. Air Force program on the MA-20B3 ram-jet engine, a pneumatic control unit designed for flight applications and containing the desired proportional-plus-integral action was installed on the engine. The results of the tests conducted on the unit are reported herein. The control unit is not a complete control system, and in the tests reported herein the unit was inserted into the system already under test in place of the electronic computer. The steady-state and

UNCLASSIFIED
[redacted]

transient performance of the control unit under simulated flight conditions was obtained, and the results are compared with those from bench tests of the control previously conducted by the manufacturer.

The controlled engine was operated at a flight Mach number of 2.5, at three altitudes, and at zero and 7° angles of attack. At zero angle of attack at each altitude, the system was subjected to transient disturbances over a range of control settings to determine the response characteristics and the stability limits of the control loop.

4051

SYMBOLS

The following symbols are used in this report:

A_1, A_2	diaphragm areas
A_3, A_4	orifice areas
C	capacitance, f
f/a	fuel-air ratio
K	control gain
K_L	loop gain
P_0'	pressure indication of total-pressure tube at tip of spike, lb/sq ft
p_c	output pressure of control unit, lb/sq ft
p_e	exhaust pressure to cell, lb/sq ft
p_i	static pressure 2 in. downstream of cowl lip (input pressure of control unit), lb/sq ft
p_r	reference pressure, lb/sq ft
p_u	pressure in control unit, lb/sq ft
p_0	free-stream static pressure, lb/sq ft
R	resistance, ohms
S	complex operator
t_d	dead time

V_c voltage from sensor and amplifier measuring, $P_{c,v}$

V_f fuel-valve-position voltage, v

V_i input voltage to fuel servomotor, v

w_f fuel flow, lb/sec

$w_{f,i}$ inner-ring manifold fuel flow, lb/sec

$w_{f,o}$ outer-ring manifold fuel flow, lb/sec

τ integrator time constant, sec

τ_{lag} lag time constant, sec

Subscript:

S complex operator

4051
CO-1 back

CONTROL UNIT

The control unit is shown in the schematic diagram of figure 1. The diaphragm areas A_1 and A_2 are connected by the shaft which varies the orifice area A_3. The system is a force-balance system; that is, it is free to move without restraint in accordance with the resultant pneumatic forces acting on the diaphragm areas A_1 and A_2. The bearing between the chambers at pressures p_i and p_u is assumed to be frictionless and to provide a good seal. The chambers at pressures p_u and p_c are connected by the integral-time-constant adjustment valve. The pressure ratio P_0'/p_e is sufficiently large and the orifice areas A_4 and A_3 are sized so that the flow through the area A_3 is always choked; thus p_c is a function only of P_0' and the shaft position.

Operation

In the operation of the control unit, any difference in pressure between p_r and p_i will give a resultant force on the shaft; for example, $p_i > p_r$ gives a force to the left. The pressures p_u and p_c are initially the same and therefore contribute no resultant forces. The shaft moves to the left, increasing the orifice area A_3 and lowering p_c. The pressure p_u cannot change immediately because of the restriction of the integrator valve; and therefore p_u is now greater than p_c, tending to give a balancing force to the right. The shaft then moves to a new balance position depending on the initial difference between p_i and p_r, which gives a change in the control output pressure p_c proportional to this difference or error signal.

The air in the chamber at pressure p_u, however, is being bled through the integrator valve to the chamber at pressure p_c. This gives a further unbalance of forces to the left and results in a continuous movement of the shaft to the left. The continuous shaft movement causes a subsequent lowering of p_c at a rate determined by the bleed characteristics of the integrator valve and the difference in pressures p_r and p_i.

4051

Transfer Function

The transfer function of the control unit may be defined as follows. If the diaphragm areas A_1 and A_2 are equal and the pressure p_r is constant for a given flight condition, the following equation may be written:

$$A_1 p_r - A_1 p_i + A_2 p_u - A_2 p_c = 0 \tag{1}$$

Differentiating equation (1) gives

$$-A_1 \,\Delta p_i + A_2 \,\Delta p_u - A_2 \,\Delta p_c = 0 \tag{2}$$

If the volume of the chamber where the pressure p_u exists is considered a capacitance and the flow of air across the integral-time-constant adjustment valve (fig. 1) is considered a resistance, then

$$\Delta p_u = \frac{\Delta p_c}{1 + RC_s} = \frac{\Delta p_c}{1 + \tau_s} \tag{3}$$

where $\tau = RC$. Substituting equation (3) in equation (2) gives

$$-A_1 \,\Delta p_i + \frac{A_2 \,\Delta p_c}{1 + \tau_s} - A_2 \,\Delta p_c = 0$$

where

$$\frac{\Delta p_c}{\Delta p_i} = -\frac{A_1}{A_2}\left(1 + \frac{1}{\tau_s}\right)$$

4051

Since the areas are equal,

$$\frac{\Delta p_c}{\Delta p_i} = -1\left(1 + \frac{1}{\tau s}\right)$$

The transfer function of the control is therefore proportional-plus-integral. The gain of the control is given by equation (1), and the integrator time constant τ is varied by a micrometer adjustment valve.

The results of a bench test by the manufacturer gave a transfer function

$$\frac{p_e - p_c}{p_i - p_r} = -e^{-0.02s}\frac{(\tau s + 1)}{\tau s(\tau_{lag,s} + 1)}$$

indicating the control to have a dead time of 0.02 second and a lag of 0.015±0.005 second in addition to the proportional-plus-integral action. The bench tests also indicated a variation of integrator time constant as a function of micrometer valve setting, as shown in figure 2.

The frequency-response curves of the control for three integrator time constants calculated by using the bench-test transfer function are shown in figure 3.

Installation

The engine variable used for control purposes was a static-pressure tap located on the vertical centerline of the inner body 2 inches downstream of the cowl lip. The connecting tubing from the pressure tap to the control unit was 40 inches of 1/4-inch tubing.

The control unit was mounted on the side of the engine in an airstream whose total temperature was 413° F. The reference pressure p_r was set manually for the particular test condition. The pressure from the control tap is p_i. A total-pressure tap at the tip of the engine spike supplied a pressure P_0', and p_e was referenced to the engine test cell. The controlled output pressure p_c was sensed by a pressure transducer. The pressure sensor converted the pressure signal from p_c into an electric signal suitable for operating an electronically excited fuel valve used in the test. In practice, the pressure signal from p_c could also control a pneumatically operated fuel valve.

Control-Loop Components

In figure 4 is shown the block diagram of the control system used for the tests. The control variable p_i is sensed at a static-pressure tap 2 inches downstream of the cowl lip. The difference in the pressure p_i and the reference pressure p_r causes the control to give a corrective pressure output p_c. The pressure p_c is converted to an electric signal by the sensor and carrier amplifier. The auxiliary computer provides a means for varying the proportional loop gain of the system and also sets a base fuel-flow level. In this investigation, the control unit was acting as a trim control about a base point set by the auxiliary computer.

The voltage v_i drives the fuel servomotor, which varies the fuel flow until p_i is equal to p_r and the control unit is balanced.

The control-loop component sensitivities are as follows:

Fuel servomotor, (lb/sec fuel flow)/v 0.520
Engine (depending on flight conditions for operating points set), (lb/sq ft)/(lb/sec fuel flow). . . . 1100-1840
Pressure sensor and carrier amplifier, v/(lb/sq ft) . . . . 0.584×10^{-3}
Computer, v/v . . . . Variable gain

APPARATUS AND INSTRUMENTATION

Engine

The 28-inch-diameter MA-20B3 ram-jet engine used in this test is shown in the cutaway drawing of figure 5. The engine was installed in a free-jet facility. Angle-of-attack variations from zero to 7° were made by varying the angle of the supersonic nozzle.

Fuel System

The fuel flow to the inner-ring fuel manifold was set at a fixed value, and all adjustments to fuel flow were made in the outer-ring fuel manifold by means of a fuel servomotor.

The fuel servomotor system contained an electrohydraulic servomotor system which positioned a throttle in a specially designed fuel-metering valve in response to an input voltage signal. The fuel-metering valve incorporated a differential relief valve, which maintained a constant pressure differential across a metering orifice. Since the metering

4051

area was a linear function of throttle position, the fuel flow was also a linear function of throttle position and of the input voltage to the fuel servomotor. This type of throttle plus reducing-valve differential-pressure regulator system is described in detail in reference 3.

The response of the fuel system, piping, and manifold was flat to 10 cps ± 5 percent with approximately 30° phase shift at 10 cps.

Instrumentation

The engine variable p_i used for control purposes was sensed with a pressure transducer (including connecting tubing) of the variable reluctance type whose response was essentially flat (± 5 percent) to 20 cps with a phase shift of 6° at 20 cps. The output pressure of the control unit p_c was also sensed with a variable-reluctance-type pressure transducer (including connecting tubing) whose response was essentially flat (± 5 percent) to 20 cps with a phase shift of 12° at 20 cps.

All steady-state and transient measurements were recorded on sensitized paper in a galvanometric oscillograph with galvanometer elements having a flat response (± 5 percent) to 100 cps with a phase shift of 15° at 100 cps. The steady-state calibration of gas pressures were obtained from mercury manometers, and fuel-flow calibrations were obtained from turbine-type flowmeters with an accuracy of ± 1 percent.

TEST PROCEDURE

Steady-State Operation

The steady-state performance of the control system was investigated by operating the engine at three altitudes, 50,000, 60,000, and 65,000 feet, for a flight Mach number of 2.5 and angles of attack of zero and 7°.

Variation of the static-pressure ratio p_i/p_0 with fuel flow is shown in figure 6. At zero angle of attack (fig. 6(a)), the set point for engine operation at each altitude was set manually at the midpoint of the curves. The set points were at p_i/p_0 of 4.04, 4.12, and 4.12 for altitudes of 50,000, 60,000, and 65,000 feet, respectively. The set points which had been selected for control operation at zero angle of attack (fig. 6(a)) were shifted to a nonlinear part of the curve at angle of attack (fig. 6(b)).

For each flight condition at the engine operating point, the control unit was operated over a range of loop gains to the point of instability, and at a single flight condition the control was operated over a range of integrator time constants.

Transient Operation

The behavior of the engine and control system during transients was investigated by means of the following series of disturbances: (1) step disturbances of fixed magnitude in input voltage V_i to fuel servomotor for varying the loop gain with constant integrator time constant (Disturbances were made at each of the three altitudes at zero and 7° angles of attack.); (2) transient disturbances in angle of attack of zero to 7° at each flight condition for integrator time constant equal to 0.045 second and fixed control gain; (3) step disturbances in V_i of constant magnitude with varying integrator time constant for fixed loop gain at an altitude of 60,000 feet and zero angle of attack. 4051

RESULTS AND DISCUSSION

Fourier Analysis of Data

Oscillograph records of the control response at an altitude of 60,000 feet and zero angle of attack for three different settings of integrator time constants were subjected to Fourier analysis (ref. 4). The oscillograph record for $\tau = 0.073$ second is shown in figure 7. The analysis was performed on the control input-pressure trace p_i and on the control output-pressure trace p_c to obtain the transfer function of the control, i.e., p_o/p_i.

The resultant frequency-response curves for three integrator-time-constant settings showed the control unit to have a transfer function of $e^{-t_d s}K\left(1 + \frac{1}{\tau s}\right)$, where $K = 0.62$ (fig. 8). The analysis of the traces showed the control unit to have a dead time of 0.01 to 0.02 second. The experimental values of τ are shown in figure 8(a), and a comparison with the values obtained from the manufacturer's bench tests are shown in figure 9 giving integrator time constants in approximate agreement with those obtained from the bench tests. The area of the cross-hatched lines represents experimental values, and the solid line represents bench-test values. Only one experimental phase-shift curve ($\tau = 0.073$) is shown in figure 8(b). Experimental phase-shift curves for the other two τ settings were not obtainable with sufficient accuracy from the Fourier analysis of the control data at the operating conditions.

4051
CO-2

The scattering in integrator-time-constant values (fig. 9) obtained from the analysis may be attributed, in part, to error in fairing a curve through the high noise level of the trace and errors in the approximation used in the Fourier analysis. Also, the scattering may be caused by operation of the control beyond its linear operating range.

Steady-State Performance

At all three altitudes for zero angle of attack, the control operated satisfactorily in steady state. The operating points set by the control are shown in figure 6(a). The point selected for the control tap location set a diffuser recovery approximately 1.5 points below the maximum. At all three altitudes and an angle of attack of 7°, the control operation was marginal for the operating points selected.

The marginal operation was, in part, due to the selection of the operating point at zero, in part, to the angle of attack. As shown in figure 6(a), the set points are at the midpoint of the engine characteristic curves, which allows for approximately equal error signals for disturbances in either direction. At an angle of attack of 7°, however, these same values of set points result in operation at very nearly the maximum operating range possible and allow no margin of controllability for any disturbance which increases the fuel flow.

In addition, the control unit was unable to provide the necessary corrective signal to reduce the fuel flow by the required amount (fig. 6). For example, at an altitude of 60,000 feet and zero angle of attack, the loop gain and integrator time constant were set at values which gave good transient response to fuel-flow disturbances. However, at an angle of attack of 7°, the maximum output from the control unit was just barely sufficient to reduce the fuel flow by the required amount. As a result, the control unit remained solidly against its lower limit (maximum orifice area A_3) with no further range of operation available to correct for disturbances which tended to increase the fuel flow.

For a given control-unit output it was possible to increase the attainable change in fuel flow by increasing the gain of the auxiliary computer. Increasing the loop gain by means of the auxiliary computer effectively increased the range of operation of the control unit and allowed it to operate within its limits. However, the increase in loop gain required to accomplish this was sufficient to exceed the stability limits of the system and resulted in sustained oscillations.

Effect of Control Constants on Stability

The effects of control constants on system stability are presented for two conditions: (1) a fixed integrator time constant with varying loop gain and (2) a fixed loop gain with varying integrator time constant.

The loop gains referred to hereinafter are the product of the control gain K and the gains of the other control-loop components as determined from their steady-state characteristics. The effects of various control constants were measured in terms of the amplitude and frequency of the oscillations observed in the V_i trace at each operating condition. 4051

The amplitude was taken as one-half the peak-to-peak value of the maximum fluctuations encountered. The frequency was measured only if a single frequency in a predominant band of frequencies was clearly discernible in the fluctuations. The stability limit, as used herein, is defined as the condition at which sustained regular oscillations occur.

The effects of varying the loop gain for a fixed integrator time constant of 0.045 second and zero angle of attack are shown for three altitudes in figure 10. The selection of τ was made on the basis of an approximate criterion for this type of system, which has been substantiated in previous work, that is, set τ approximately equal to the system dead time. In this system, the dead time varied from 0.04 to 0.06 second but was usually approximately 0.045 second, as shown in figure 7 (from point A on the trace of V_i to point C on the trace of P_c).

At an altitude of 50,000 feet at zero angle of attack (fig. 10(a)), the fuel oscillation amplitude increased with loop gain until a region of instability was reached for loop-gain values between 1.04 and 1.21, oscillations being sustained at a loop gain of 1.21 with a frequency of 5.5 to 6.2 cps at this point.

For the 60,000-foot altitude at zero angle of attack (fig. 10(b)), a region of instability existed at loop-gain values of 1.65 to 1.77. Oscillations were sustained at a loop gain of 1.77 with a frequency of 5.7 cps.

For an altitude of 65,000 feet at zero angle of attack (fig. 10(c)), a region of instability occurred between loop-gain values of 1.55 and 1.66. Oscillations were sustained at 1.66 with a frequency of 6.2 cps.

4051

CO-2 back

The calculated and experimental frequency-response curves of the complete open-loop system for τ of 0.045 second, zero angle of attack, and 60,000-foot altitude are shown in figure 11. The calculated response was obtained from the engine and fuel-system experimental data cascaded with the response calculated from the manufacturer's transfer function for the control. The experimental amplitude response was obtained from the engine and fuel-system experimental data cascaded with the control experimental data. Experimental phase shift, absent from figure 11(b), was not available.

Use of the calculated amplitude ratio and phase shift resulted in a calculated stability limit at a loop gain of 2.13 and a frequency of 4.5 cps. Since the phase shift was not available for calculation of the stability limit from the experimental frequency response, the frequency at instability obtained experimentally (4 to 6.3 cps, fig. 10(b)) was used to determine the normalized amplitude existing at instability (0 to 0.58 from fig. 11(a)). The experimental loop gain at instability was then obtained by determining the factor necessary to increase the normalized amplitude to a value of unity. The experimental loop gain at instability determined in this manner was 1.85 to 2.17.

The effect of integrator time constant on stability limits was determined at an altitude of 60,000 feet at zero angle of attack with the loop gain held constant at 0.828. The value of loop gain selected was that which provided the best response for τ equal to 0.045 second, which will be discussed in the following section. The integrator time constant was varied from 0.024 to 0.073 second. Figure 12 shows that, as the integrator time constant was decreased below 0.033 second, the control became unstable. Oscillations were sustained for an integrator-time-constant setting of 0.024 second with a frequency of 4.4 to 5 cps.

Response to Step Disturbance

The effects of various control constants on the response characteristics of the system were also observed for the following conditions: (1) a fixed integrator time constant of 0.045 second with varying loop gain and (2) a fixed loop gain with varying integrator time constant.

The response characteristics measured were the response time and the percentage of overshoot for a step disturbance in the input voltage which caused a step disturbance in fuel flow. The response time as used herein is defined as the time from initiation of a disturbance until 90 percent of the error has been initially corrected. Overshoot is defined as the ratio of the maximum overshoot occurring during the transient to the magnitude of the initial disturbance, expressed in percentage form.

In figure 7 is shown an oscillograph trace of the response of the various variables to a step disturbance in fuel flow. The trace shows a step disturbance at an altitude of 60,000 feet and zero angle of attack for an integrator time constant of 0.073 second at a loop gain of 0.828. The disturbance was a step decrease in fuel flow of 0.130 pound per second (decrease in fuel-air ratio of 0.0045). The letter A indicates the start of the step. Approximately 0.025 second later, the pressure p_i responds to the step (point B); and 0.02 second later, the controlled output pressure p_c (point C) responds. 4051

Transient response times for step disturbances in fuel flow are shown for altitudes of 60,000 and 65,000 feet at zero angle of attack in figure 13. The curves show response time and percentage of overshoot for a step size in fuel flow of ±0.130 pound per second (f/a of ±0.0045) at an altitude of 60,000 feet (f/a of engine operating point, 0.068). At an altitude of 65,000 feet, the step size in fuel flow was ±0.104 pound per second (f/a of ±0.0046) and the fuel-air ratio for the engine operating point was ±0.069. No data were available for an altitude of 50,000 feet for which the step size in fuel flow was ±0.208 pound per second (f/a of ±0.005) and the fuel-air ratio of the engine operating point was 0.076. The control settings at this condition were such that the control unit limited because of the size of the disturbance.

At an altitude of 60,000 feet (fig. 13(a)), the response time decreased rapidly as the loop gain increased until it reached a value of approximately 0.10 second at a loop gain of 1.77. With increased values of loop gain, the overshoot increased rapidly until the stability limit was reached at a loop gain of 1.77. For an altitude of 65,000 feet (fig. 13(b)), the response time decreased with loop gain to approximately 0.08 second at a loop gain of 1.0. With increased values of loop gain, the overshoot increased, reaching approximately 100 percent at a loop gain of 1.23.

Response data for a variation in integrator time constant at an altitude of 60,000 feet and zero angle of attack are shown in figure 14. This figure shows that the response time increased with increasing time constant and the percentage of overshoot decreased with increasing values of integrator time constant. A difference between overshoots for step increases and decreases may also be seen in figure 14. This difference could be caused by several factors: (1) variation of the engine sensitivity as the operating point shifts during the transient, (2) variations in control operation, and (3) variation in engine dynamics to step increases and decreases.

For altitudes of 60,000 and 65,000 feet that gave the most satisfactory control operation, the integrator time constant was 0.045 second with a control loop gain equal to 0.83, which gave a response time of approximately 0.1 second with 20-percent overshoot.

Response to Angle-of-Attack Disturbances

A trace of a ramp increase in angle of attack from zero to 7° is shown in figure 15 for an altitude of 60,000 feet, a loop gain of 0.828, an integrator time constant of 0.045 second, and zero angle of attack. The time of the ramp was 0.78 second. The letter A on the trace indicates the start of the ramp and B indicates the end of the ramp.

4051

The maximum output from the control unit was just barely sufficient to reduce the fuel flow by the required amount to bring the diffuser pressure ratio p_i/p_0 back to the set point, as indicated on the trace by the letter C. Note that the control input-pressure traces and control output-pressure traces have crossed. As a result of the control operating at its maximum output, no further range of operation was available to correct for disturbances which tended to increase the fuel flow at a 7° angle of attack.

At 50,000- and 65,000-foot altitudes, similar ramps caused the control unit to limit. At the 60,000-foot altitude and a 7° angle of attack, increasing the control loop gain to 2.36 by means of the auxiliary computer allowed the control unit to operate within its limits but resulted in sustained oscillations.

SUMMARY OF RESULTS

The following results were obtained from the investigation of the Marquardt shock-positioning control unit on a simulated flight operation of a ram-jet engine.

An analysis of the control unit showed it to be of the proportional-plus-integral type. A Fourier analysis of the control transient responses at flight conditions verified the analysis giving integrator time constants in approximate agreement with those obtained from the bench tests. The gain of the control unit was found to be 0.62 and the recorder traces showed a dead time for the control unit of 0.01 to 0.02 second.

The control unit operated satisfactorily at zero angle of attack during steady-state conditions at 50,000, 60,000, and 65,000 feet and during transient conditions at 60,000 and 65,000 feet. At angle of attack for all three flight conditions, the control unit limited for steady-state and transient conditions.

Transient disturbances at altitudes of 60,000 and 65,000 feet for zero angle of attack had approximately the same size fuel steps and the same engine operating points. The control unit at these two flight conditions had approximately the same percentage of overshoot and response time at the same loop gain. At an altitude of 50,000 feet the fuel steps were larger and the engine operating point was higher so that the control limited. No data were available for response time and percentage of overshoot at this altitude.

For the flight condition of 60,000-foot altitude, zero angle of attack, and integrator time constant of 0.045 second, the calculated stability limit of the control loop was at a loop gain of 2.27 and a frequency of 4.6 cps compared with the experimental stability limit of the control loop obtained at loop-gain values of 1.85 to 2.17 and an oscillation frequency of 4.5 to 5.8 cps. 4051

The total dead time of the components of the control loop was 0.04 to 0.06 second, and the operation of the control unit was at the most satisfactory point when the integrator time constant was 0.045 second and the loop gain equal to 0.83, resulting in a response time of approximately 0.1 second with 20-percent overshoot.

Lewis Flight Propulsion Laboratory
National Advisory Committee for Aeronautics
Cleveland, Ohio, May 18, 1956

REFERENCES

1. Hurrell, Herbert G., Vasu, George, and Dunbar, William R.: Experimental Study of Shock-Positioning Method of Ram-Jet-Engine Control. NACA RM E55F21, 1955.

2. Vasu, George, Hart, Clint E., and Dunbar, William R.: Preliminary Report on Experimental Investigation of Engine Dynamics and Controls for a 48-Inch Ram-Jet Engine. NACA RM E55J12, 1956.

3. Otto, Edward W., Gold, Harold, and Hiller, Kirby W.: Design and Performance of Throttle-Type Fuel Controls for Engine Dynamic Studies. NACA TN 3445, 1955.

4. Delio, Gene J.: Evaluation of Three Methods for Determining Dynamic Characteristics of a Turbojet Engine. NACA TN 2634, 1952.

4051

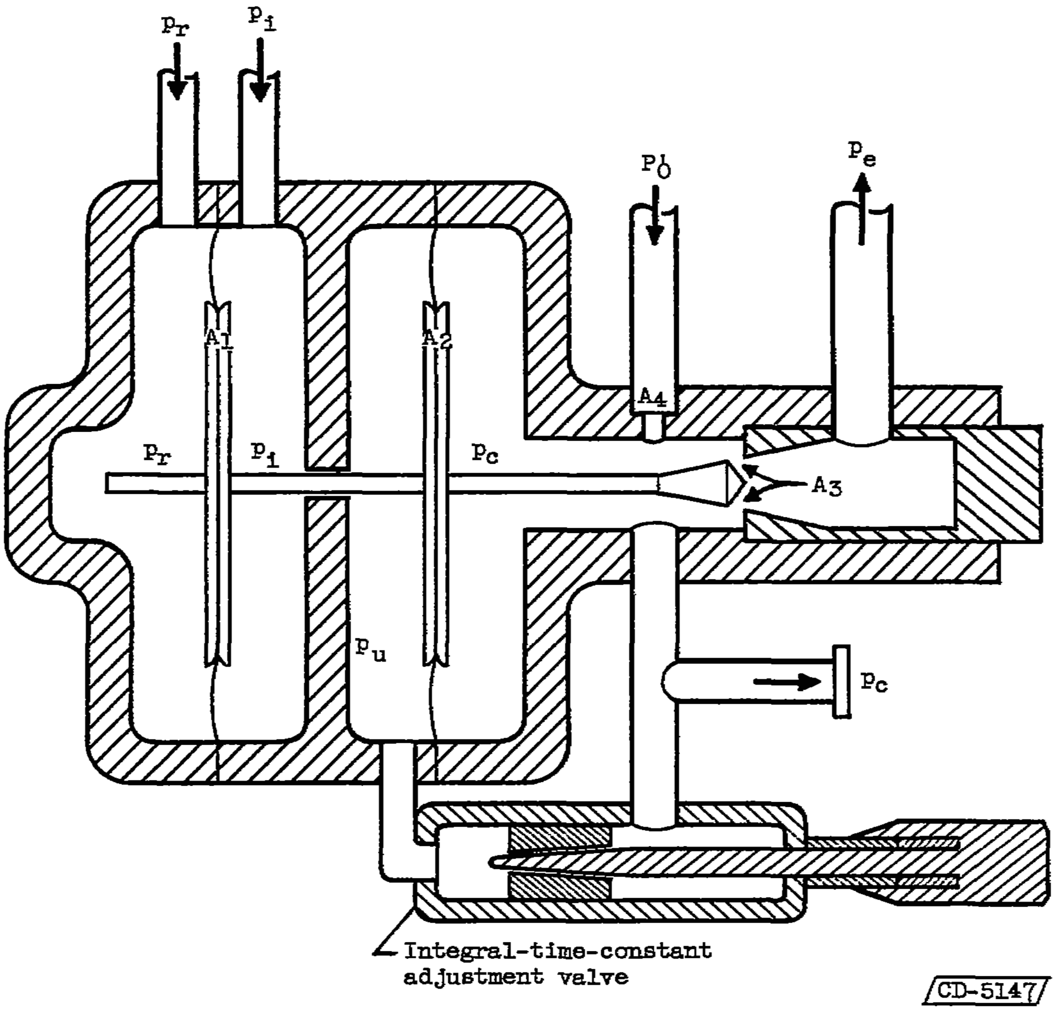

Figure 1. - Schematic diagram of proportional-plus-integral shock-positioning control unit.

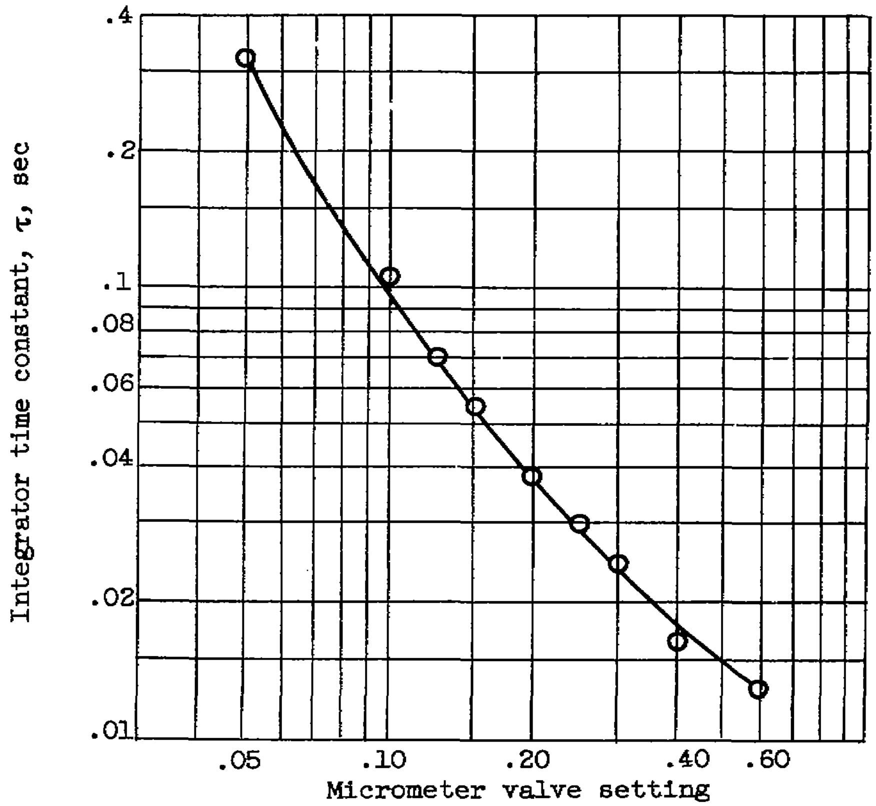

Figure 2. - Bench test of integrator time constant as function of micrometer valve setting.

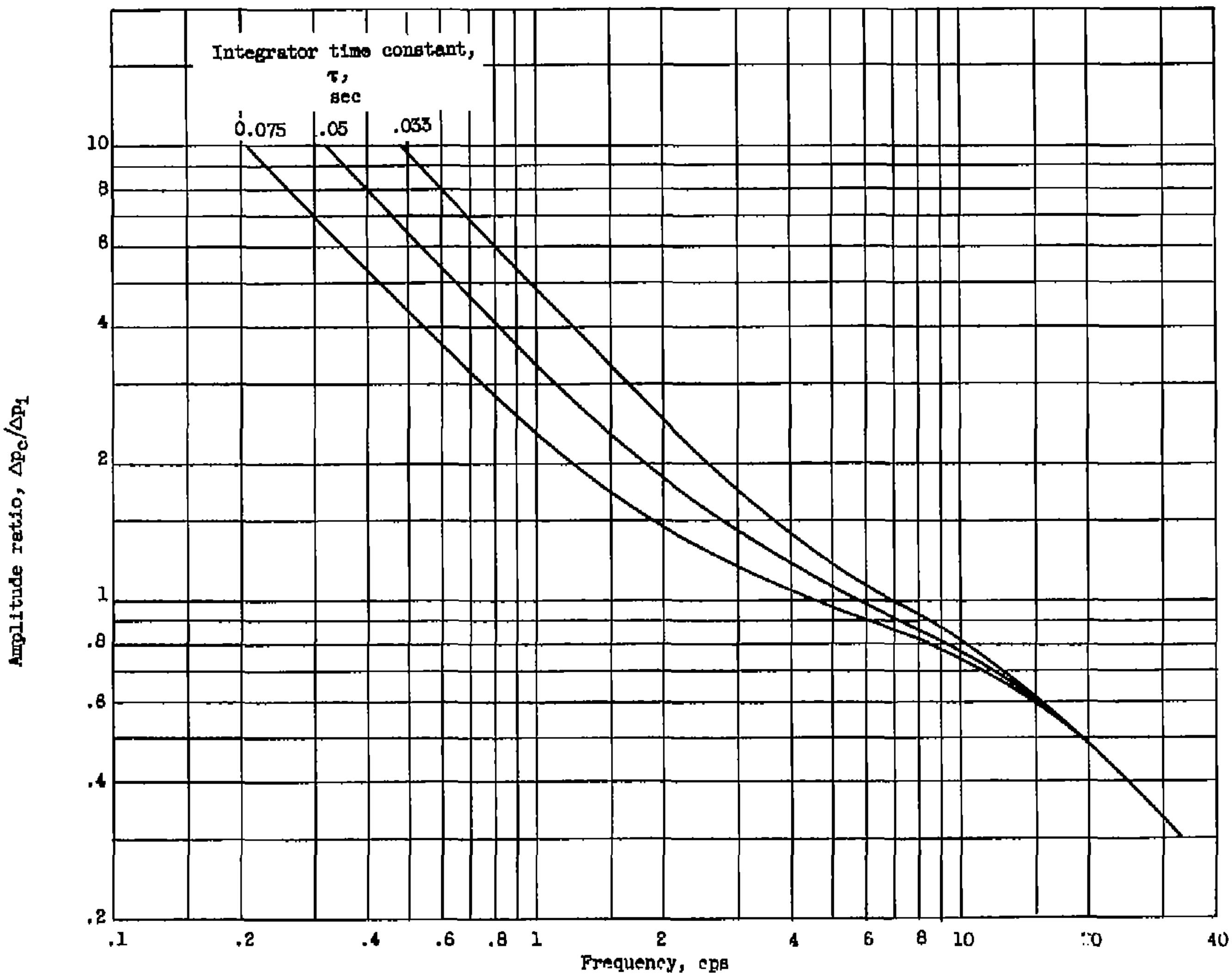

(a) Amplitude ratio.

Figure 3. - Bench-test calculated frequency response of control unit for various integrator time constants.

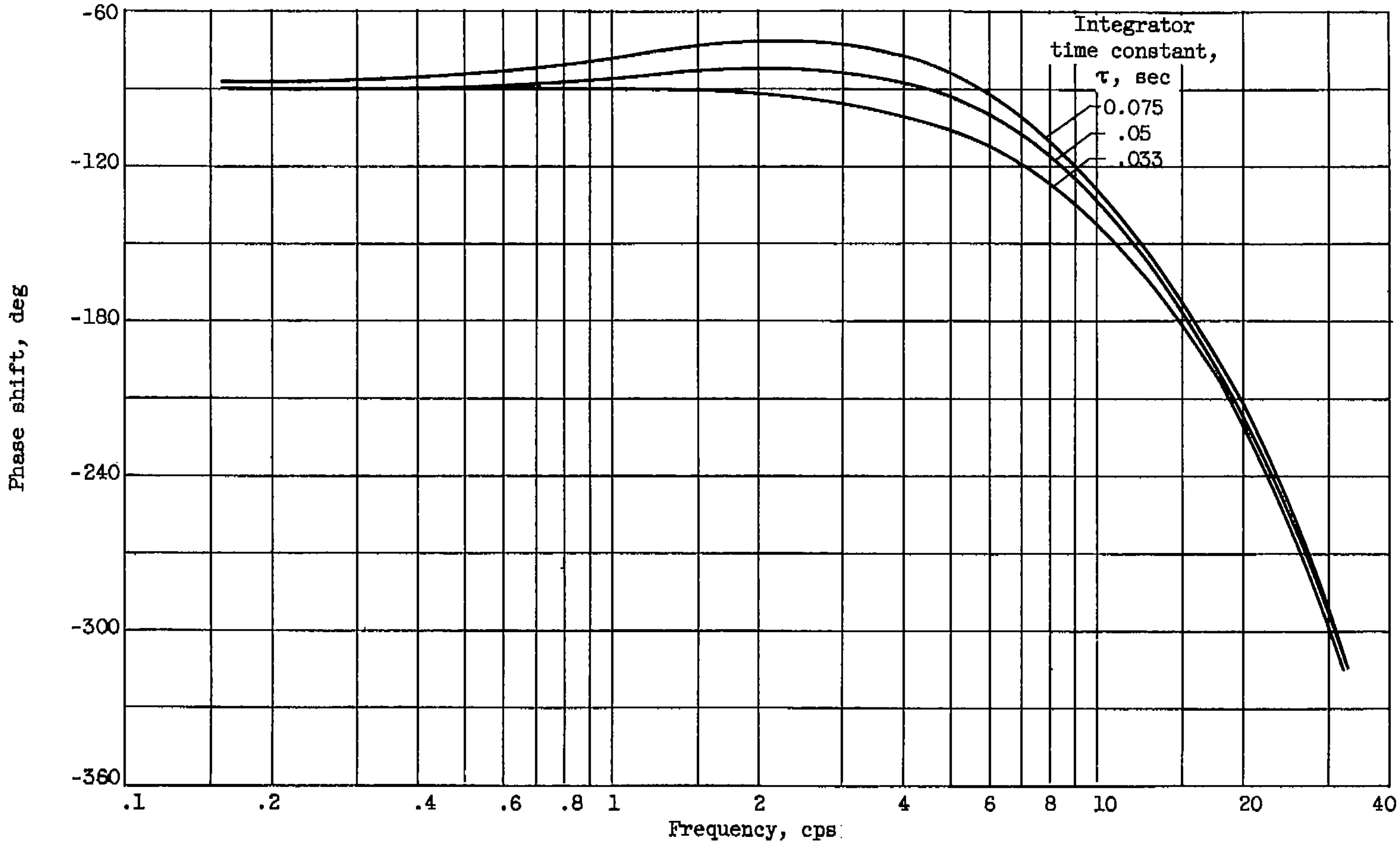

(b) Phase shift.

Figure 3. - Concluded. Bench-test calculated frequency response of control unit for various integrator time constants.

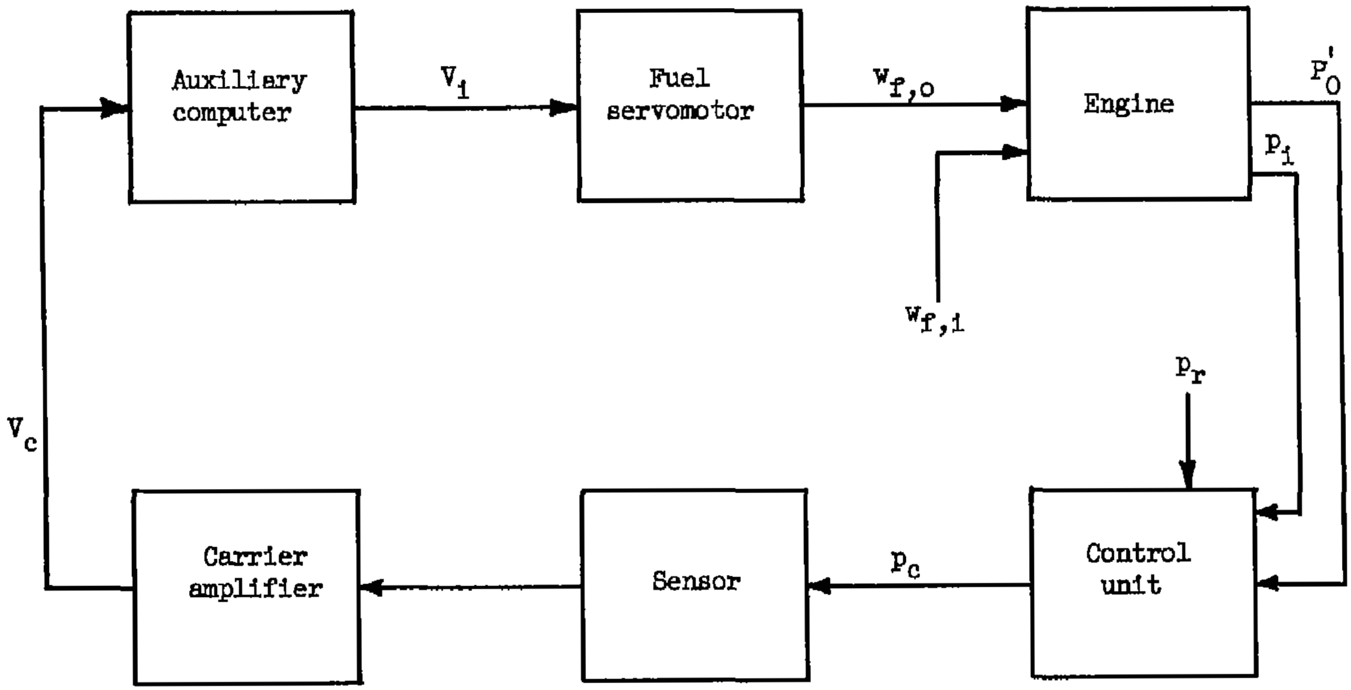

Figure 4. - Block diagram of control loop.

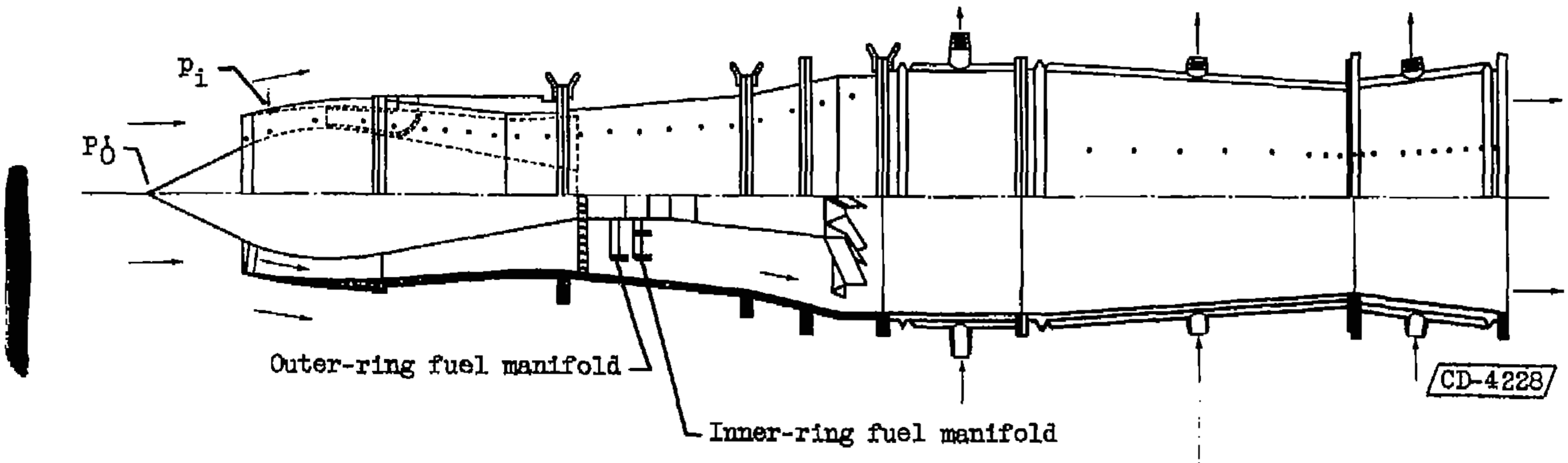

Figure 5. - Cross-sectional view of 28-inch-diameter MA-20B3 ram-jet engine.

4051

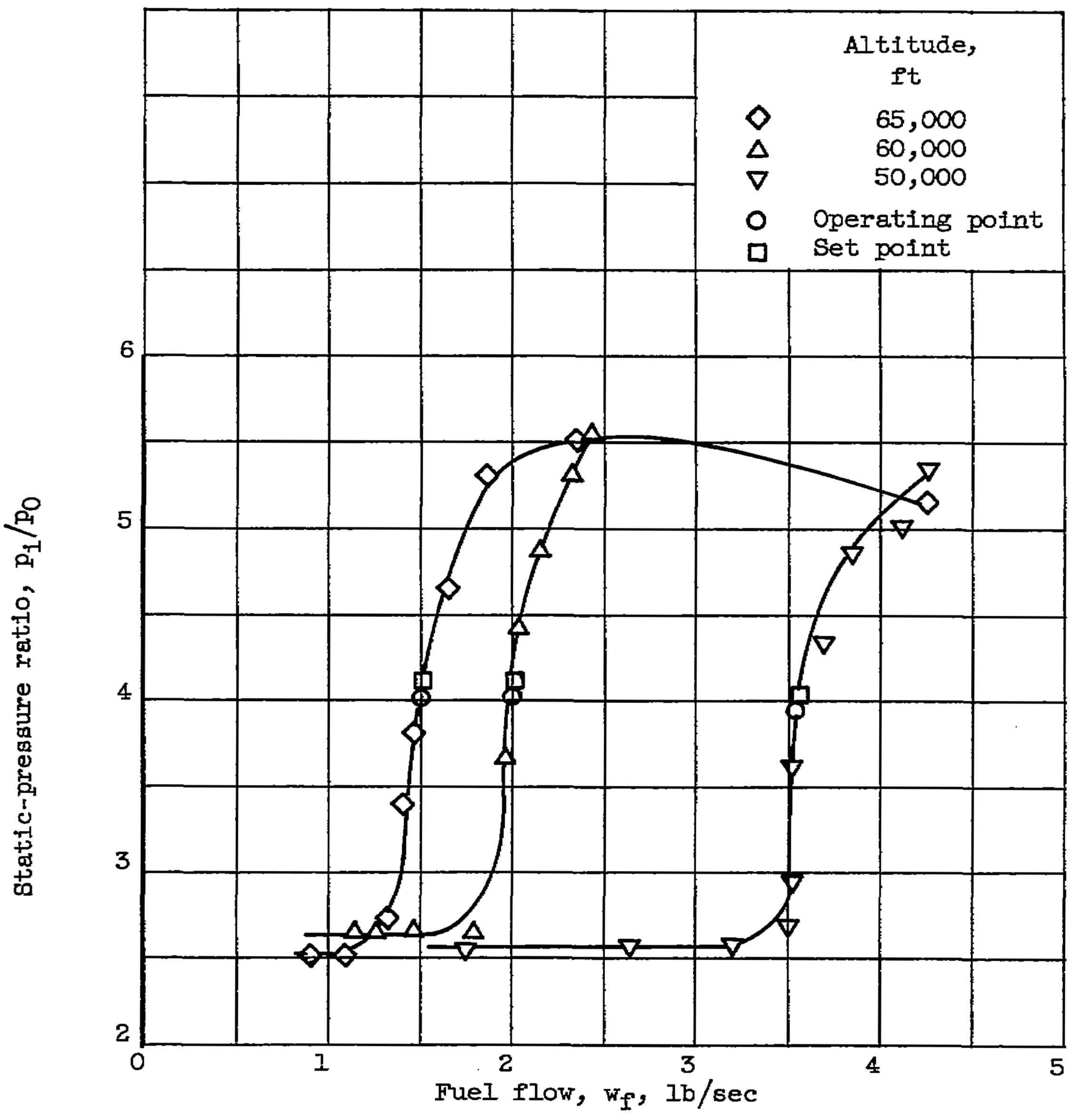

(a) Zero angle of attack.

Figure 6. - Variation of static-pressure ratio with fuel flow. Flight Mach number, 2.5.

[redacted]

4051

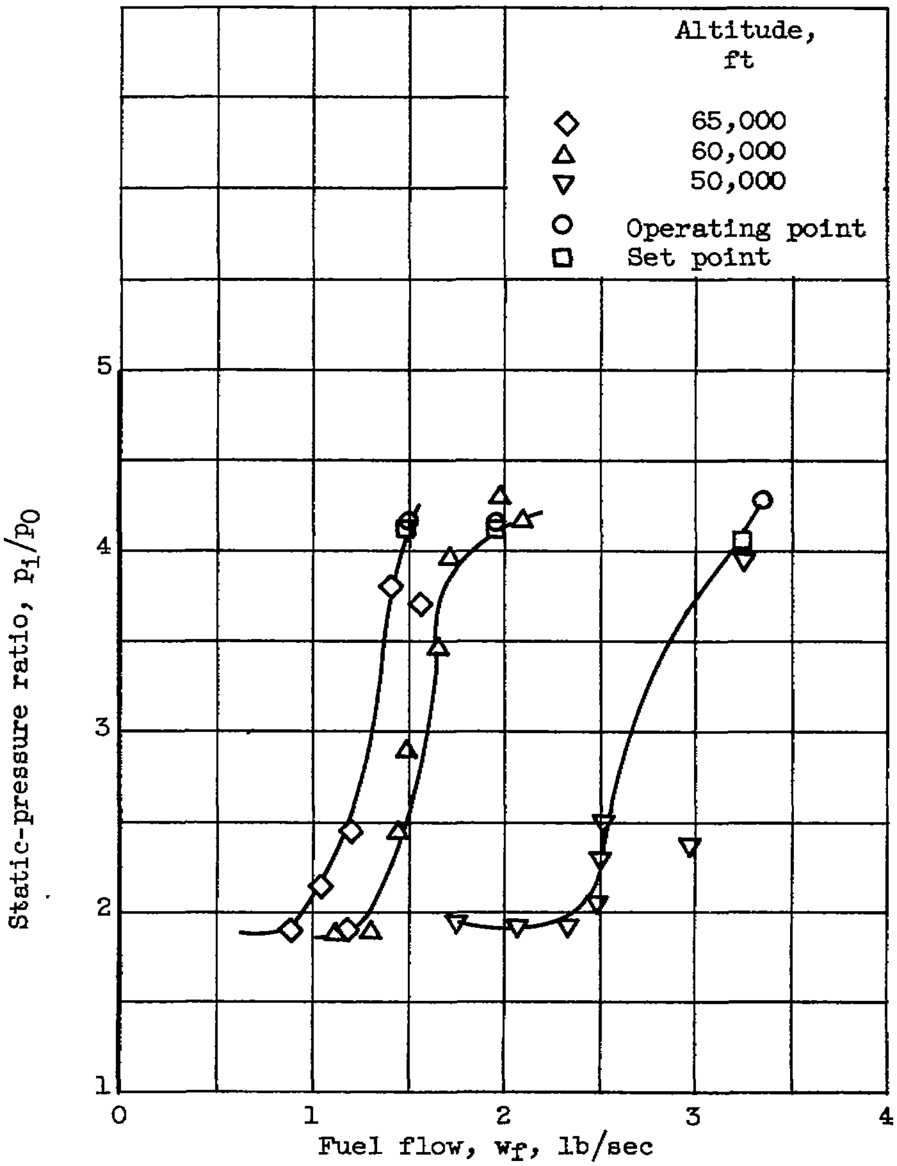

(b) Angle of attack, 7°.

Figure 6. - Concluded. Variation of static-pressure ratio with fuel flow. Flight Mach number, 2.5.

[redacted]

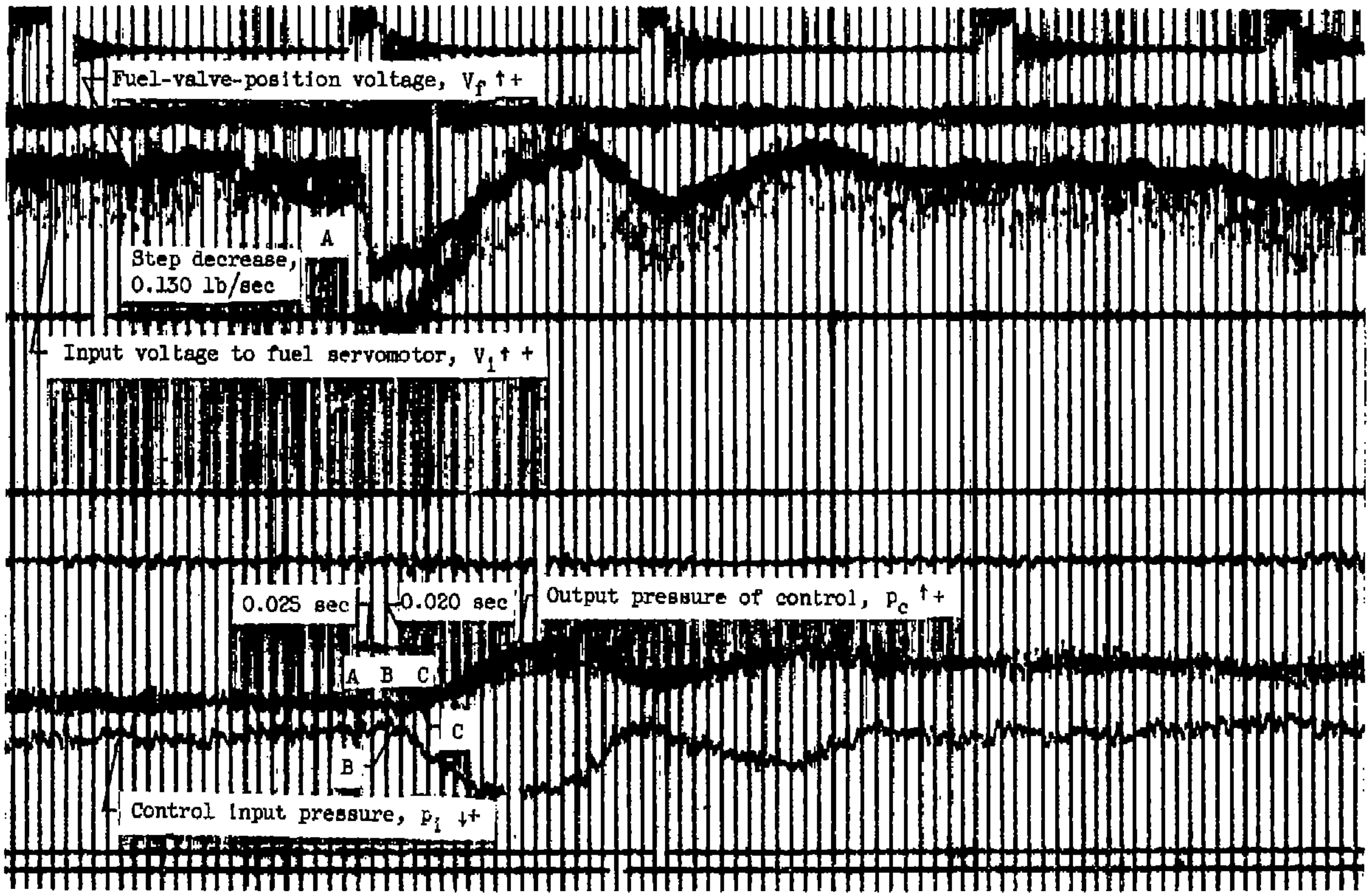

Figure 7. - System response to step decrease in fuel flow. Flight Mach number, 2.5; altitude, 60,000 feet; zero angle of attack; integrator time constant, 0.073; loop gain, 0.828.

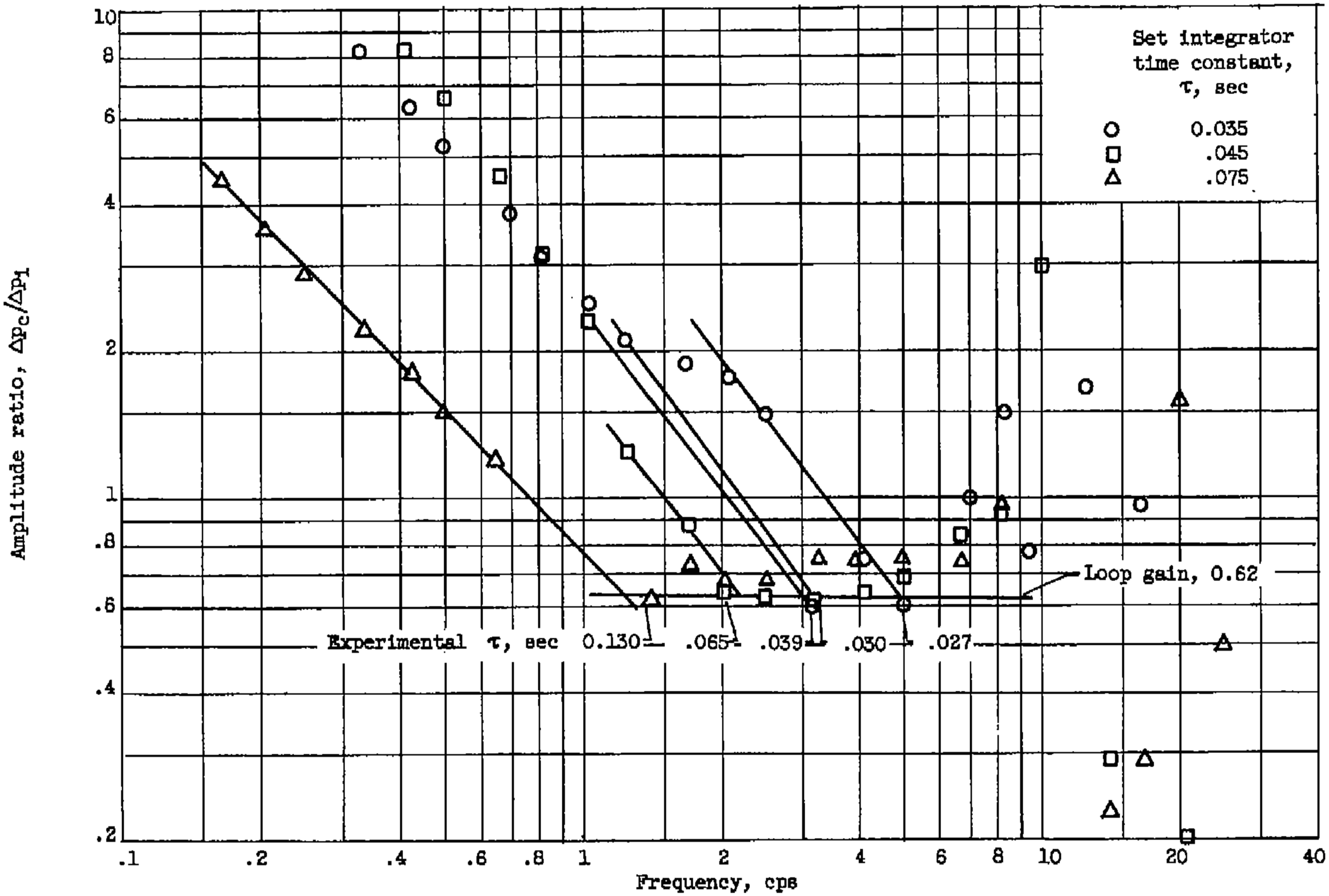

(a) Amplitude ratio.

Figure 8. - Experimental frequency response of control unit from Fourier analysis.

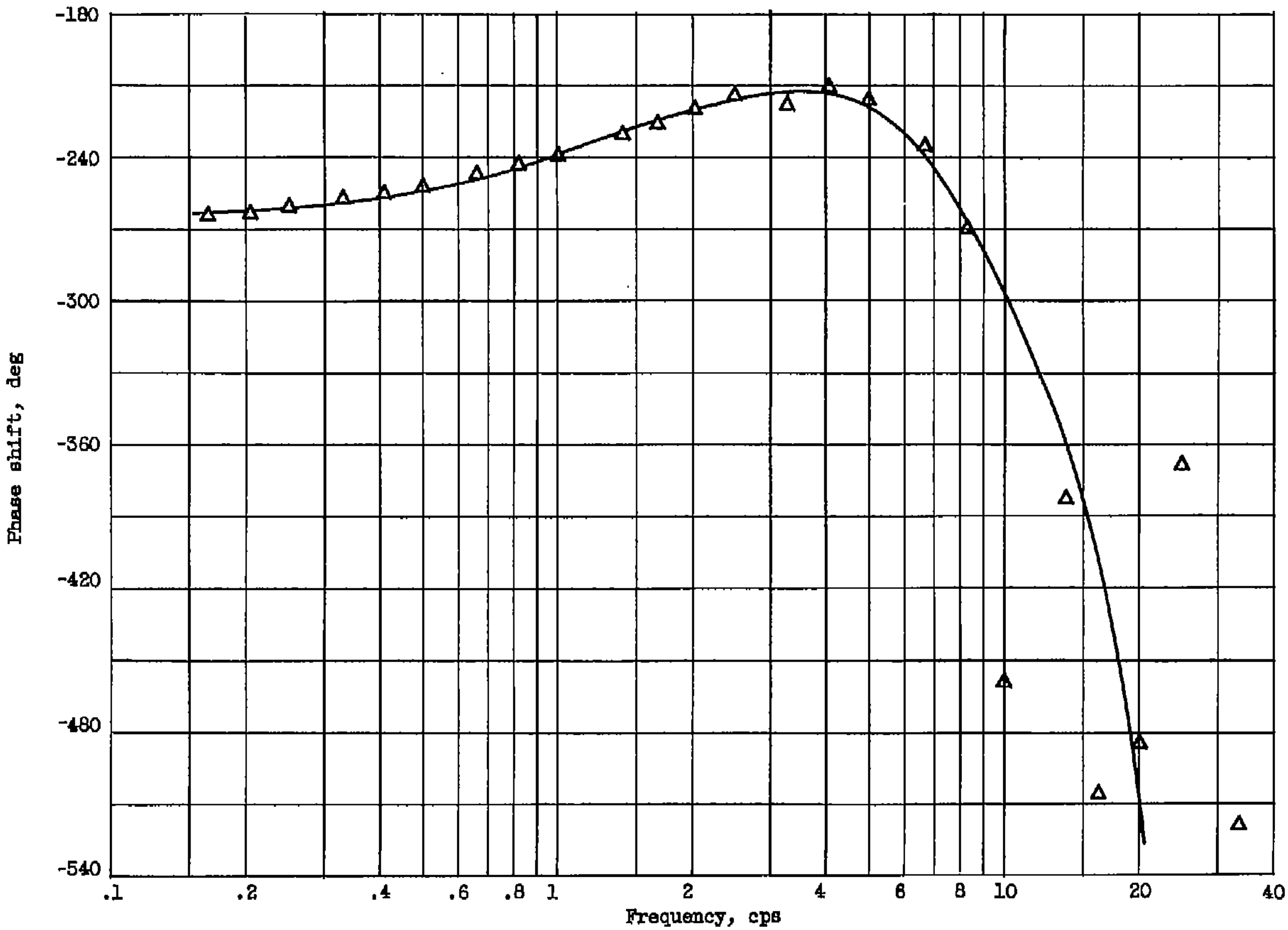

(b) Phase shift. Integrator time constant, 0.073 second.

Figure 8. - Concluded. Experimental frequency response of control unit from Fourier analysis.

4051

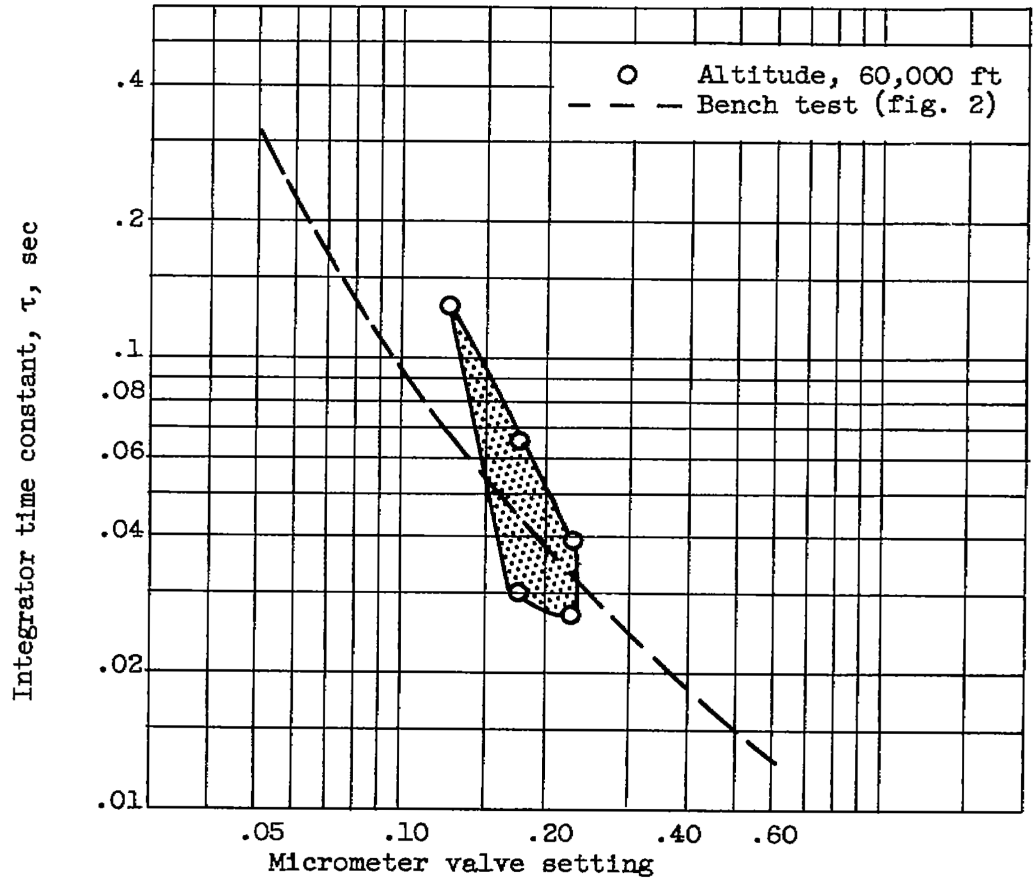

Figure 9. - Integrator time constant as function of micrometer setting.

4051

CO-4 back

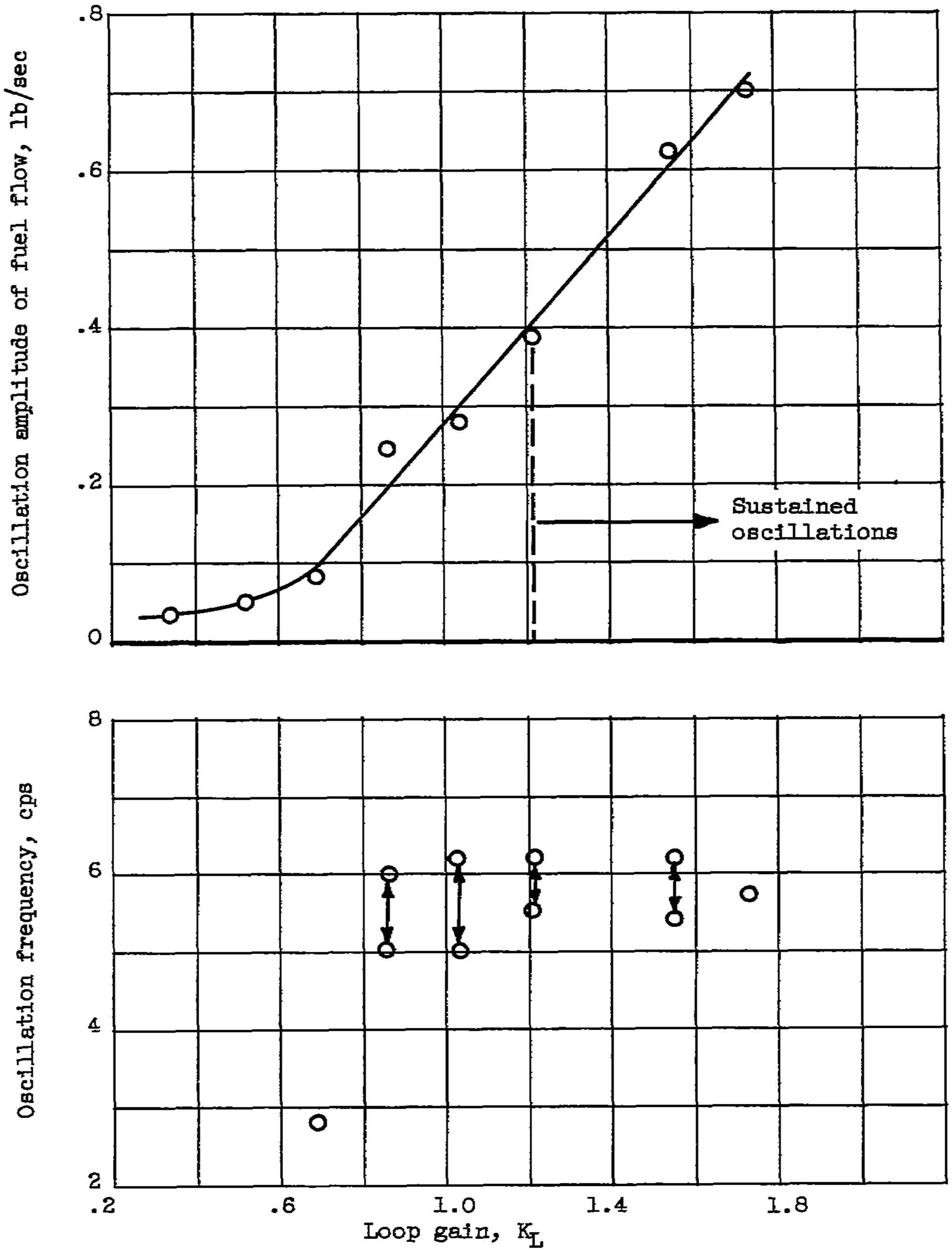

(a) Altitude, 50,000 feet; operating point, 3.99.

Figure 10. - Oscillation amplitude and frequency as function of loop gain. Flight Mach number, 2.5; zero angle of attack; integrator time constant, 0.045.

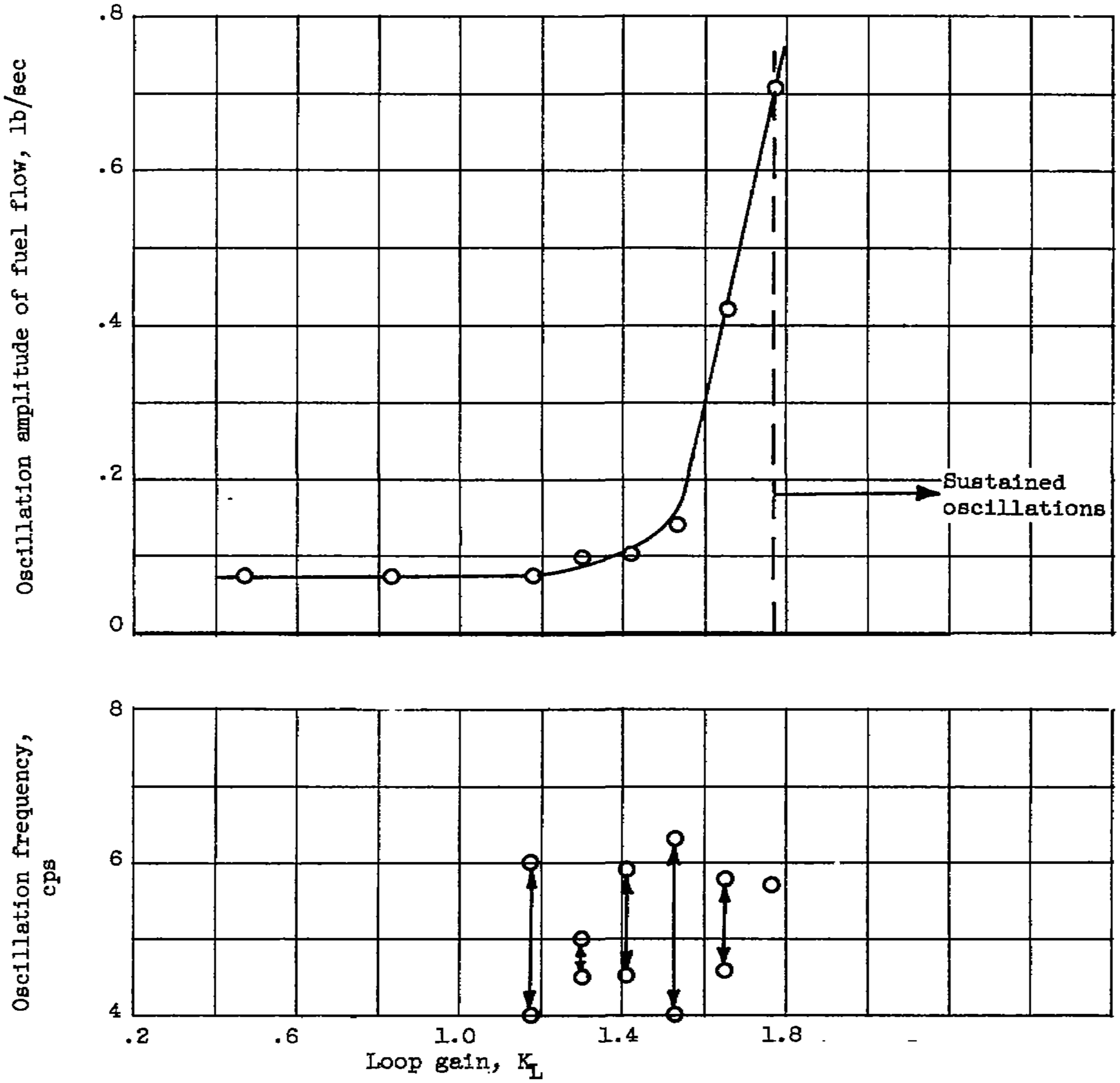

(b) Altitude, 60,000 feet; operating point, 4.02.

Figure 10. - Continued. Oscillation amplitude and frequency as function of loop gain. Flight Mach number, 2.5; zero angle of attack; integrator time constant, 0.045.

4051

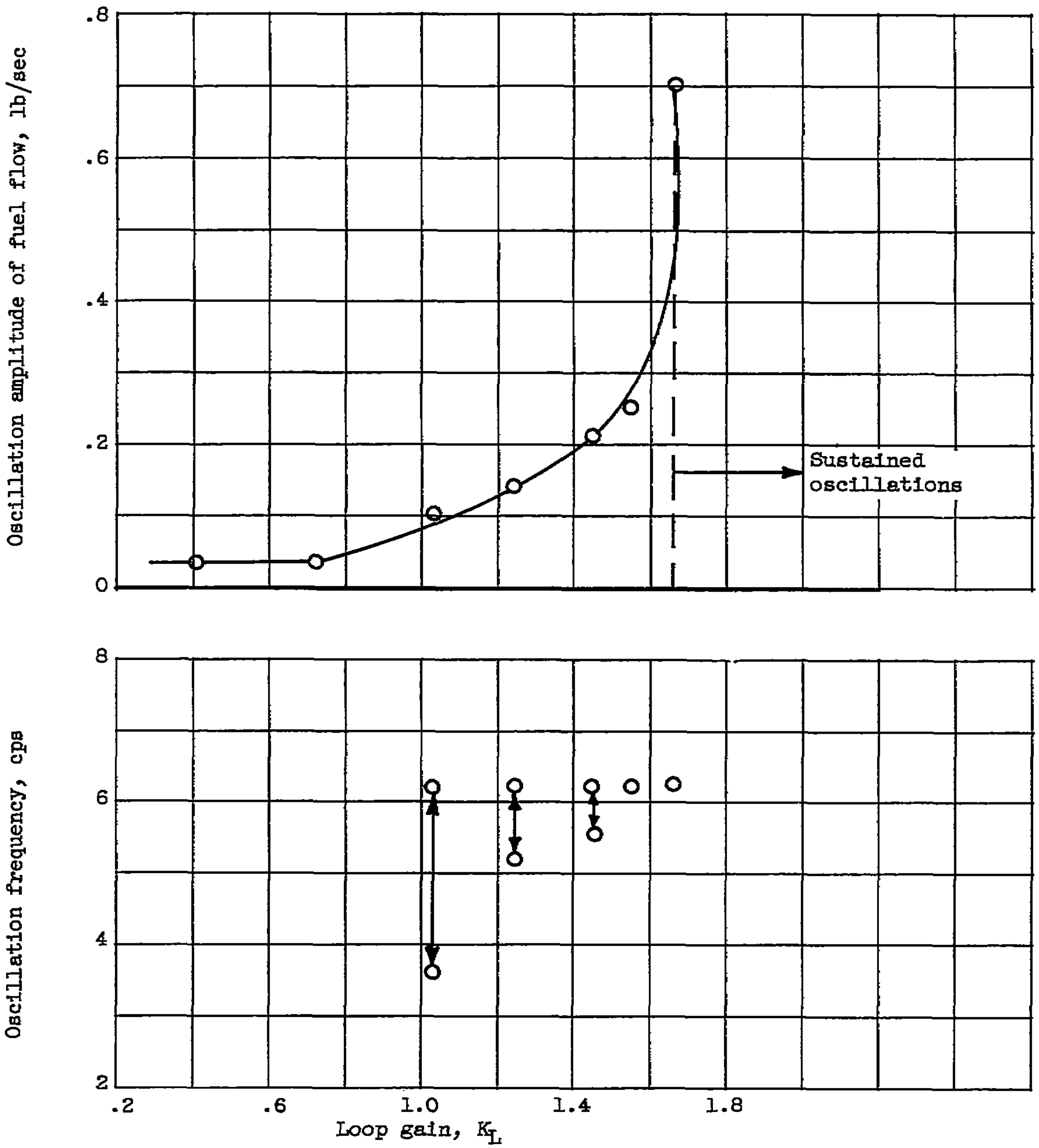

(c) Altitude, 65,000 feet; operating point, 4.03.

Figure 10. - Concluded. Oscillation amplitude and frequency as function of loop gain. Flight Mach number, 2.5; zero angle of attack; integrator time constant, 0.045.

[redacted]

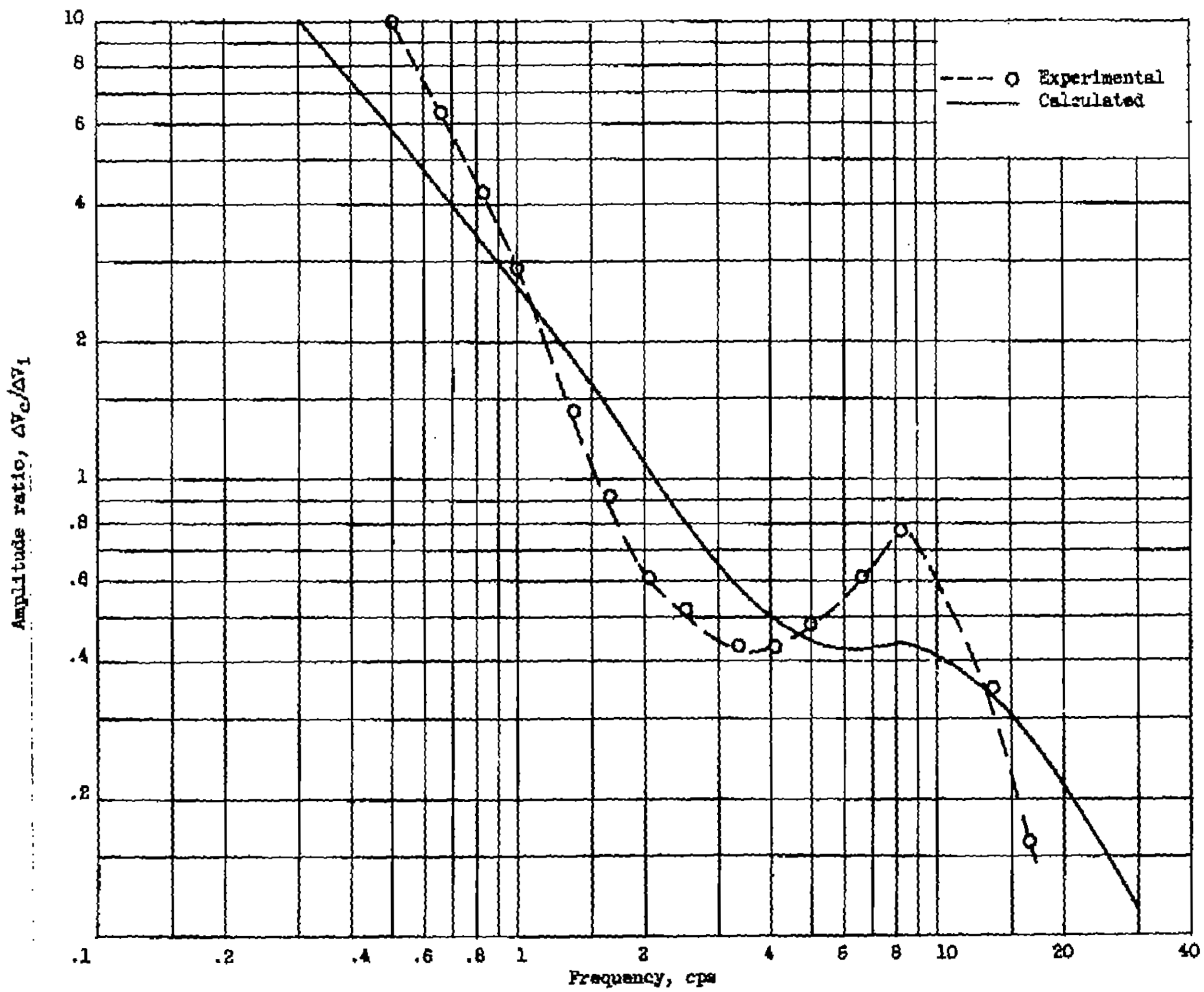

(a) Calculated and experimental; amplitude ratio.

Figure 11. - Frequency-response curves of open-loop system. Flight Mach number, 2.5; altitude, 60,000 feet; zero angle of attack; integrator time constant, 0.045 second; operating point 4.05.

[redacted]

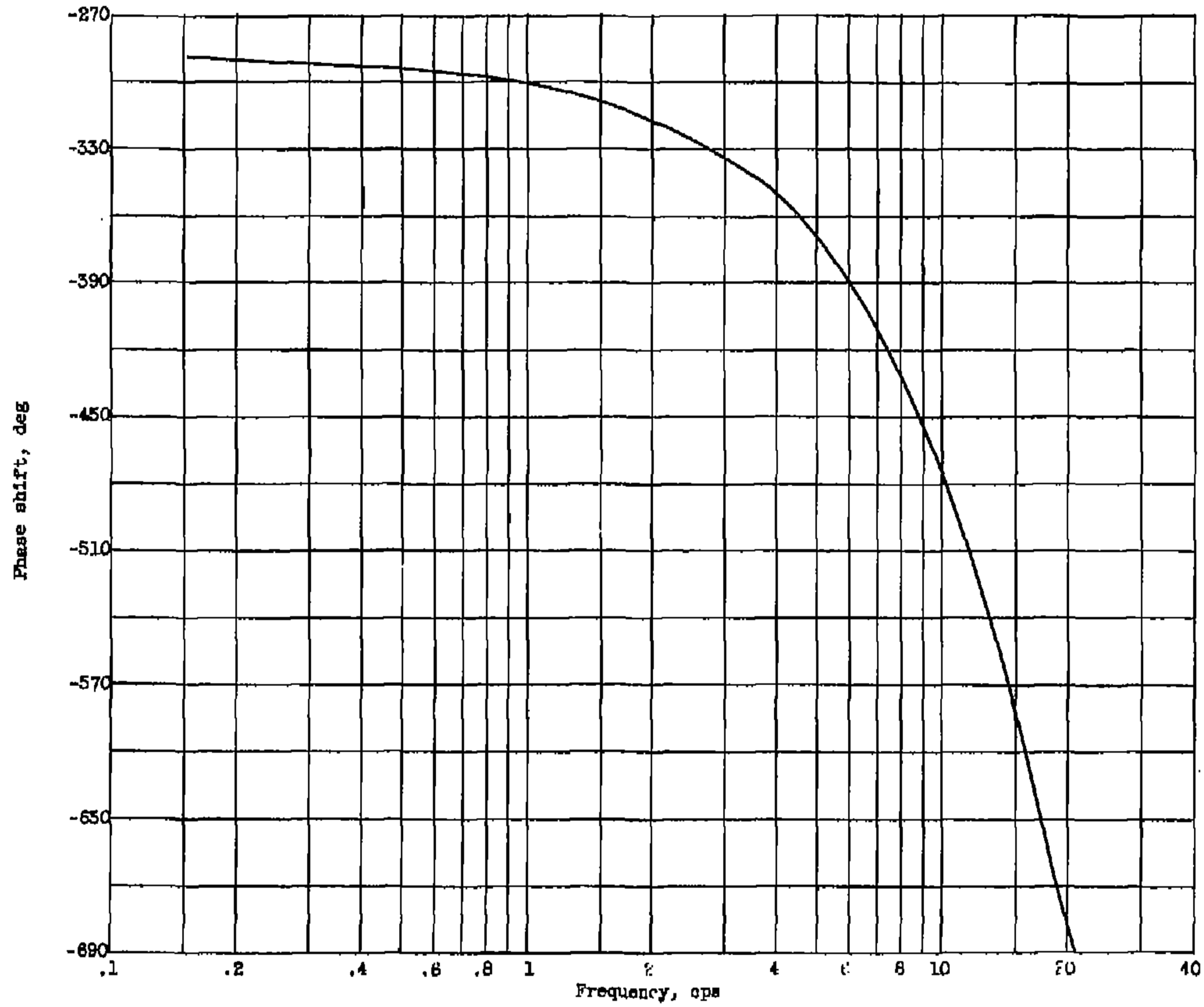

(b) Calculated; phase shift

Figure 11. - Concluded. Frequency-response curves of open-loop system. Flight Mach number, 2.5; altitude, 60,000 feet; zero angle of attack; integrator time constant, 0.045 second; operating point, 4.05.

4051

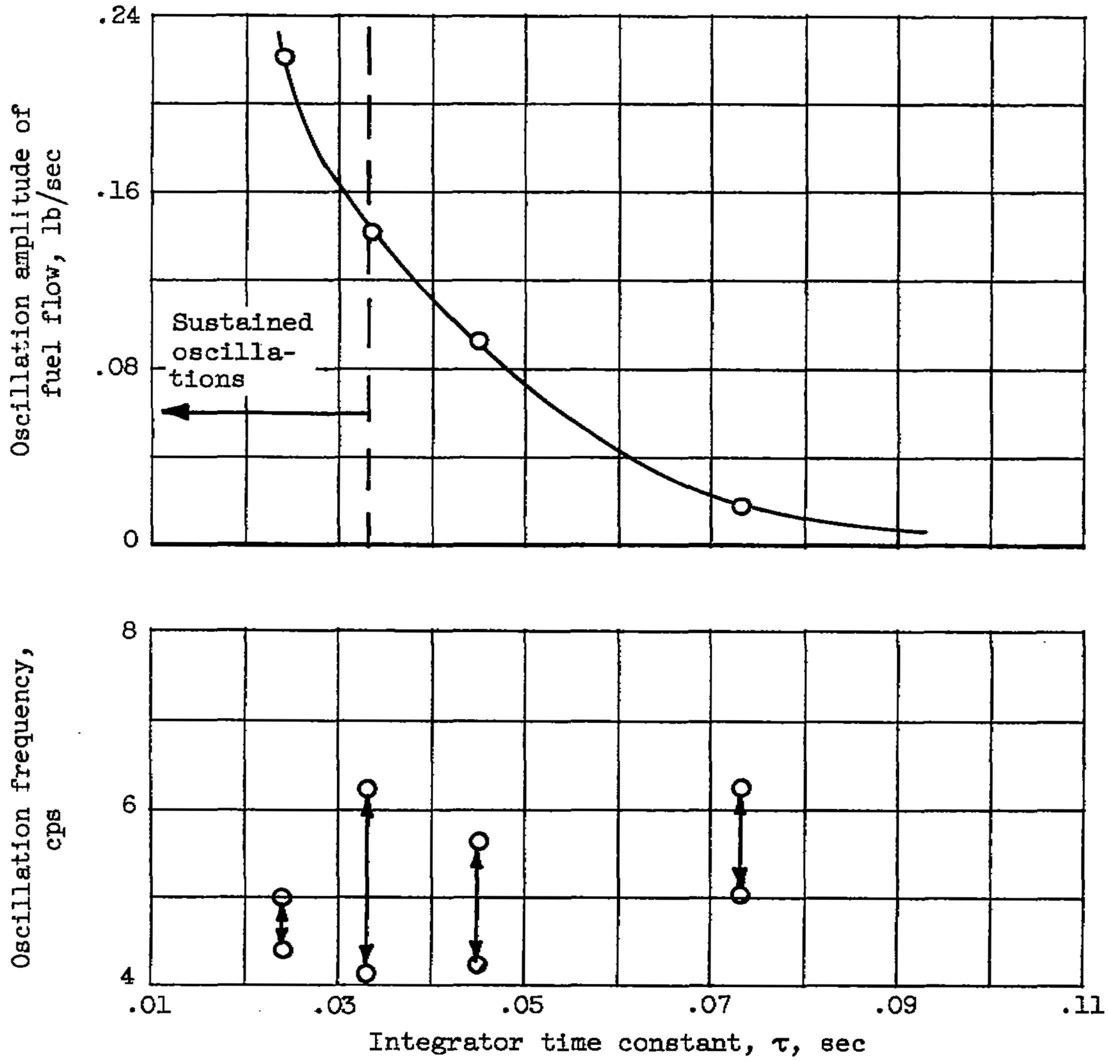

Figure 12. - Oscillation amplitude and frequency as function of integrator time constant. Flight Mach number, 2.5; altitude, 60,000 feet; zero angle of attack; loop gain, 0.828; operating point, 4.05.

[redacted]

4051

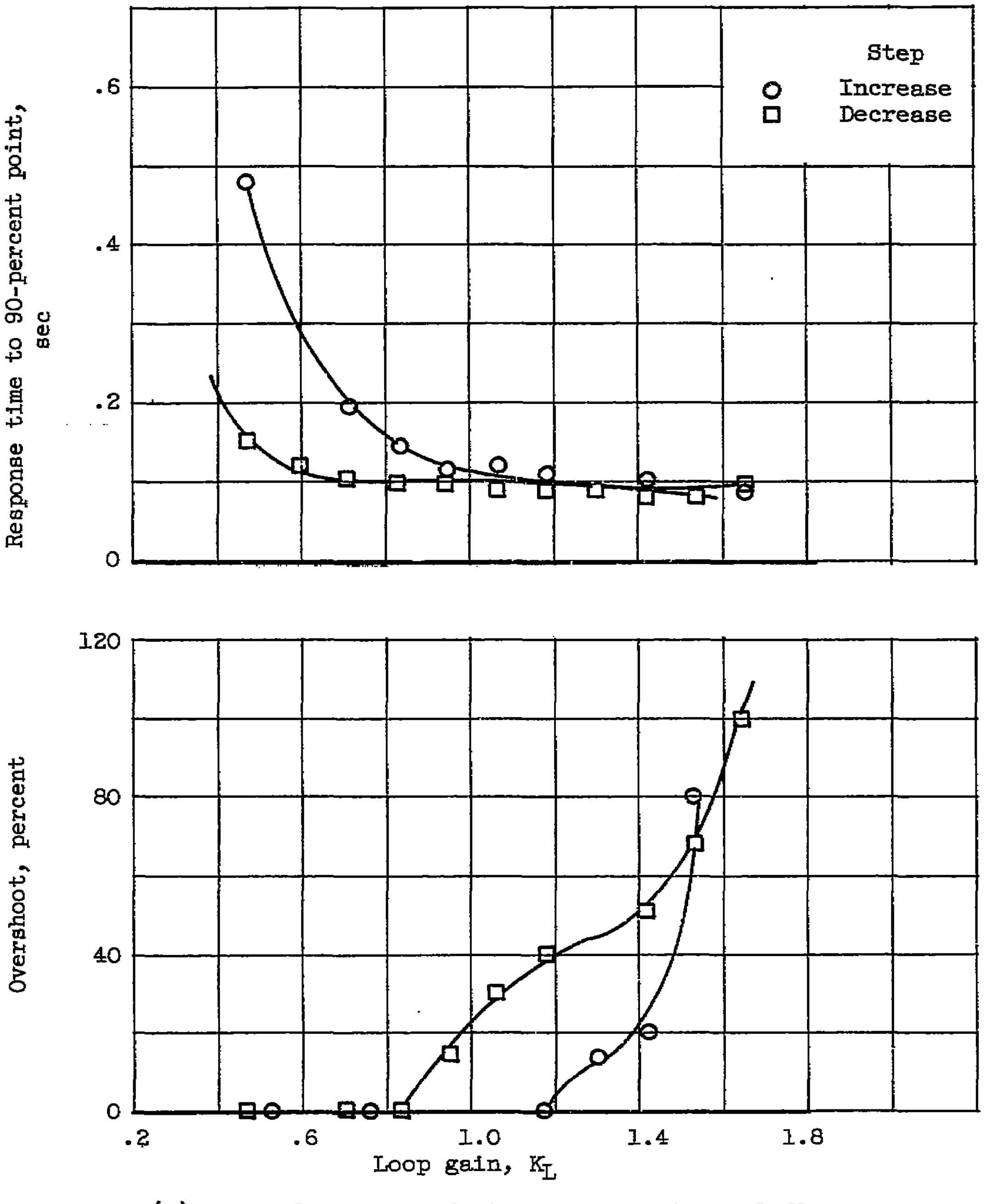

(a) Altitude, 60,000 feet; step size in fuel flow, ±0.130 pound per second (fuel-air ratio, ±0.0045).

Figure 13. - System response to step disturbance in fuel flow. Flight Mach number, 2.5; zero angle of attack; integrator time constant, 0.045 second; operating point, 4.03.

[redacted]

4051

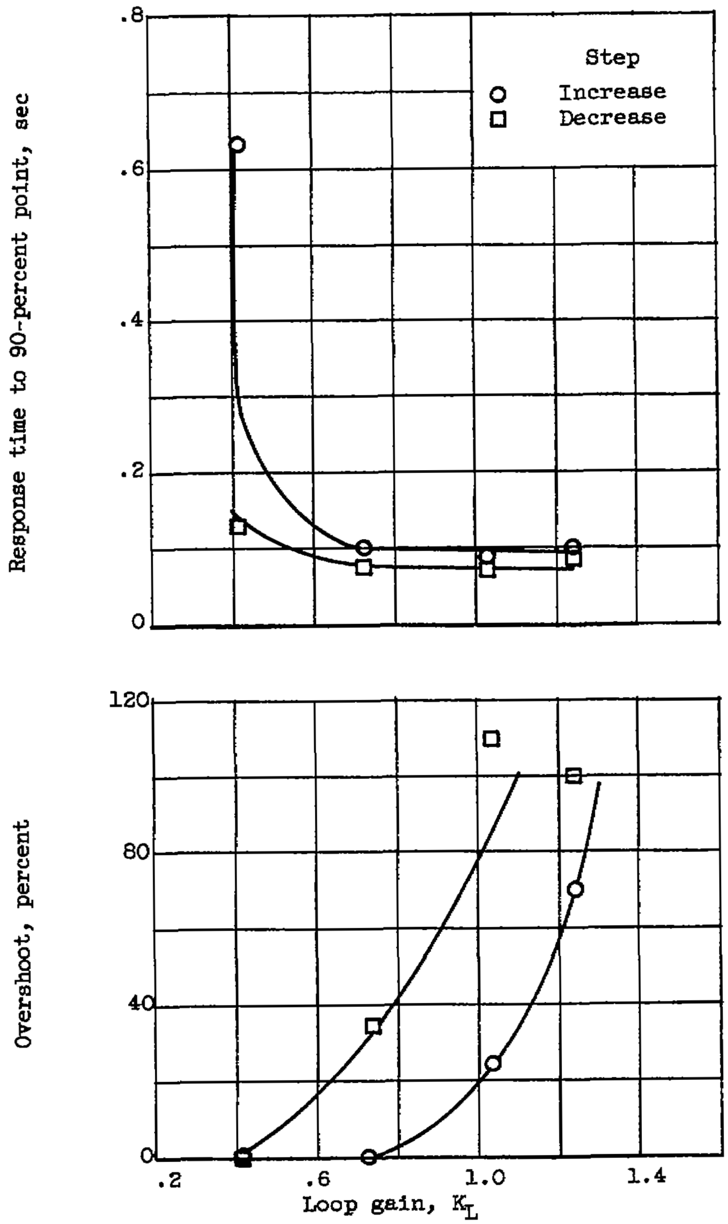

(b) Altitude, 65,000 feet; step size in fuel flow, ±0.104 pound per second (fuel-air ratio, ±0.0046).

Figure 13. - Concluded. System response to step disturbance in fuel flow. Flight Mach number, 2.5; zero angle of attack; integrator time constant, 0.045 second; operating point, 4.03.

[redacted]

4051

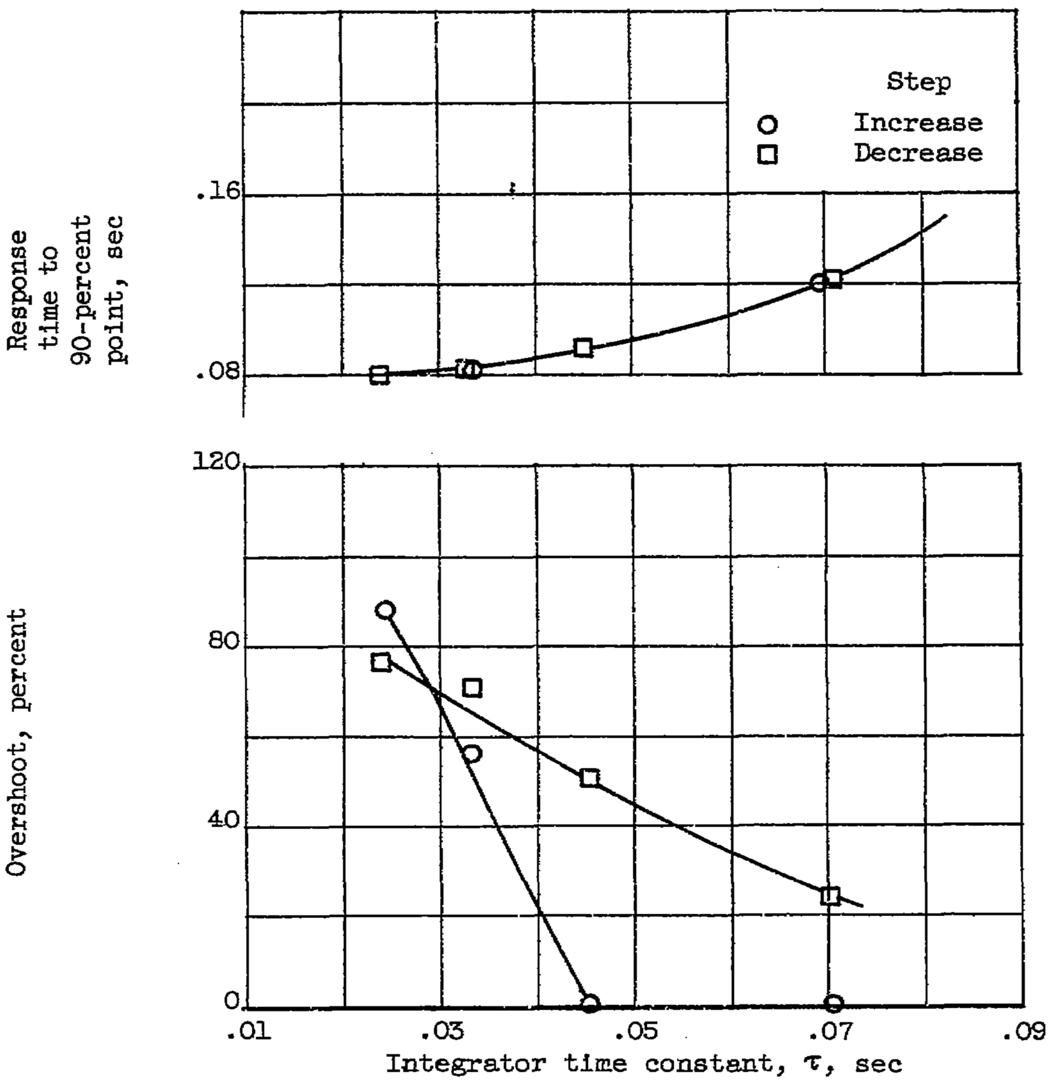

Figure 14. - System response to step disturbance in fuel flow. Flight Mach number, 2.5; altitude, 60,000 feet; zero angle of attack; loop gain, 0.828; operating point, 4.03; step size in fuel flow, ±0.130 pound per second (fuel-air ratio, ±0.005).

[redacted]

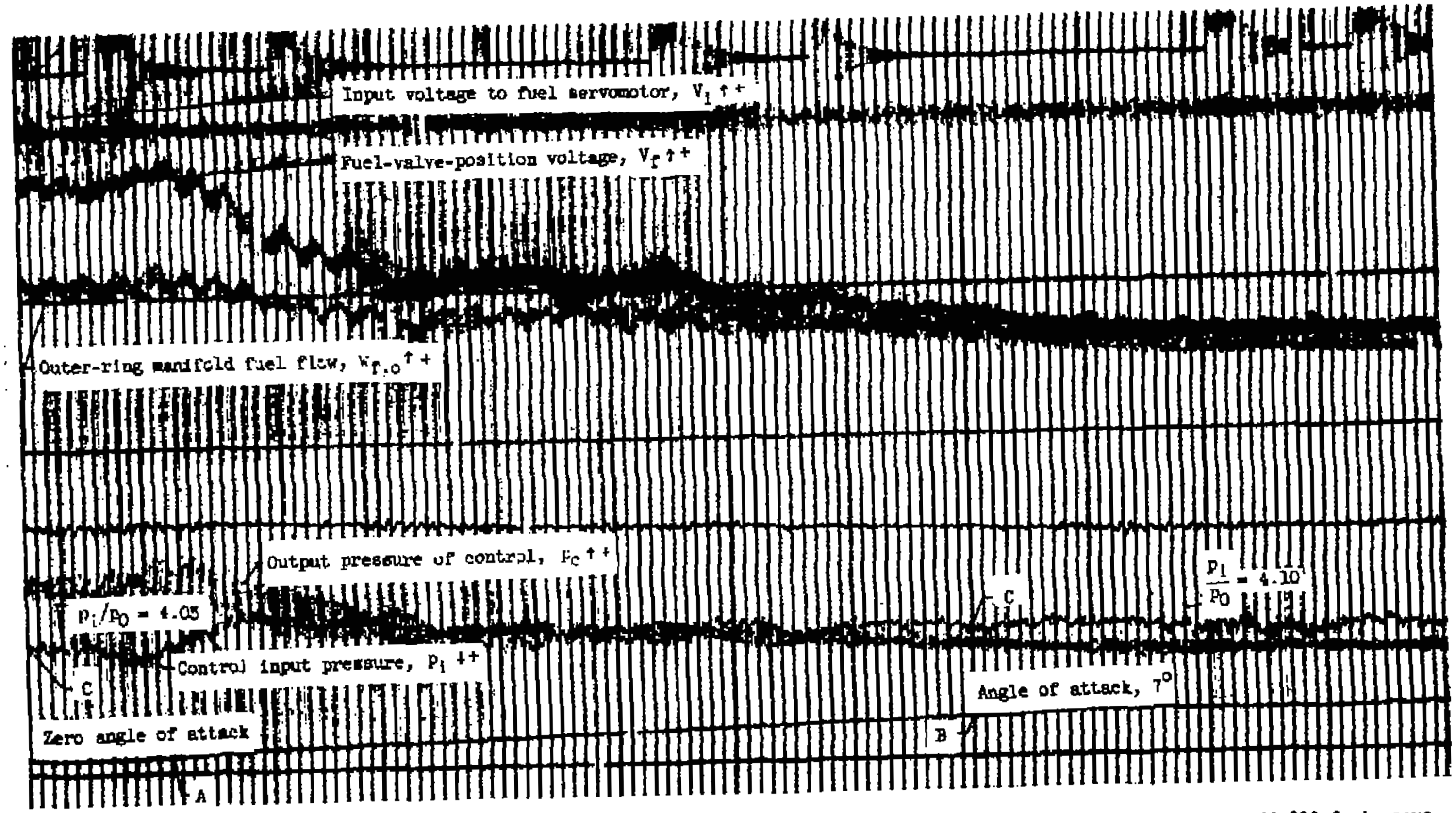

Figure 15. - System response to ramp increase in angle of attack from zero to 7°. Flight Mach number, 2.5; altitude, 60,000 feet; zero angle of attack; loop gain, 0.828; integrator time constant, 0.045 second.

NASA Technical Library
3 1176 01435 8528